Original

Crueger, T.; Kuhnert, H.; Paetzold, J.; Zorita, E.:

Calibrations of Bermuda corals against large-scale SST- and SLP-pattern time series and implications for climate reconstructions

In: Journal of Geophysical Research (2006) AGU

DOI: 10.1029/2005JD006903

JOURNAL OF GEOPHYSICAL RESEARCH, VOL. 111, D23103, doi:10.1029/2005JD006903, 2006

Calibrations of Bermuda corals against large-scale sea surface temperature and sea level pressure pattern time series and implications for climate reconstructions

T. Crueger,[1] H. Kuhnert,[2] J. Pätzold,[2] and E. Zorita[1]

Received 21 November 2005; revised 13 June 2006; accepted 8 August 2006; published 12 December 2006.

[1] Proxy records from stony reef corals are established tools for reconstructing climate features. However, validation procedures for proving the calibrations are often insufficient or even lacking. We address this problem by the establishment and validation of statistical regression models for the reconstruction of large-scale climate patterns from local coral records (upscaling). We apply the upscaling technique to the annual growth rates of two coral species from Bermuda, representing a period of about 140 years. The coral records are related to reanalyzed sea surface temperature (SST) and sea level pressure (SLP) fields. In the western North Atlantic, the correlation maps between the SSTs and the single coral records and their leading principal component show similar structures. On the basis of regression patterns for limited areas, upscaling models are established. Validation of such models for the SST yields an explained variance of 30% of the low-pass-filtered data using the first principal component of both corals. For the detrended SLP time series, representing an almost hemispheric SLP pattern, 21% of the interannual variability is explained by means of only one coral. Thus different corals from neighboring sites represent similar climate signals, however, to slightly varying degrees, leading to different reconstruction skills. Problems remain in reconstructing long-term trends. We conclude that reconstructions from multiple corals are not a priori predominant to those from single corals. A calibration to what extent a single coral represents a climate parameter should be the first step before combining multiple corals as the basis for a reconstruction.

Citation: Crueger, T., H. Kuhnert, J. Pätzold, and E. Zorita (2006), Calibrations of Bermuda corals against large-scale sea surface temperature and sea level pressure pattern time series and implications for climate reconstructions, *J. Geophys. Res.*, *111*, D23103, doi:10.1029/2005JD006903.

1. Introduction

[2] The understanding of climate and its variability requires long-time data sets far beyond the time of instrumental data. Where instrumental data are missing or data coverage is insufficient, proxy data derived from paleoclimatic archives are used to obtain climatic information. Corals represent an extensively used archive providing century-long, annually or seasonally resolved records from the shallow tropical and subtropical oceans. The most commonly measured coral proxies for sea surface temperature (SST) include δ^{18}O [*Pätzold*, 1984; *McConnaughey*, 1989; *Kuhnert et al.*, 1999; *Felis et al.*, 2000; *Gagan et al.*, 2000], Sr/Ca [*Smith et al.*, 1979; *Alibert and McCulloch*, 1997; *Linsley et al.*, 2004; *Felis et al.*, 2004], and skeletal extension rates [*Dodge and Vaišnys*, 1975; *Slowey and Crowley*, 1995; *Lough and Barnes*, 1997; *Carricart-Ganivet*, 2004]. δ^{18}O is also an indicator for sea surface salinity (SSS) and precipitation [*Cole and Fairbanks*, 1990; *Linsley et al.*, 1994; *Cobb et al.*, 2003; *Pfeiffer et al.*, 2004; *Timm et al.*, 2005].

[3] Most investigations on coral proxies are confined to correlations or calibrations against local SST or rainfall time series or large-scale climate indices, such as the NAO or NIÑO3 indices. Only a few of these investigations performed a validation check, i.e., tested the proxy calibration against independent data [*Crowley et al.*, 1999; *Quinn and Sampson*, 2002; *Lough*, 2004]. *Crowley et al.* [1999] calibrated seasonally and annually resolved δ^{18}O against local gridded SSTs and performed a validation with independent data. Besides underlining the need of verification against independent data, they recommended calibrations against large-scale fields in order to relate coral proxies to large-scale climate signals. *Lough* [2004] standardized coral stable isotope data and gridded SST series for a 30-year period. By applying this standardization to the remaining periods of the data, verification against independent data was performed. It was found that although most of the coral time series show significant relationships with interannual

[1] GKSS Research Centre, Geesthacht, Germany.
[2] Department of Geosciences, University of Bremen, Bremen, Germany.

0148-0227/06/2005JD006903$09.00

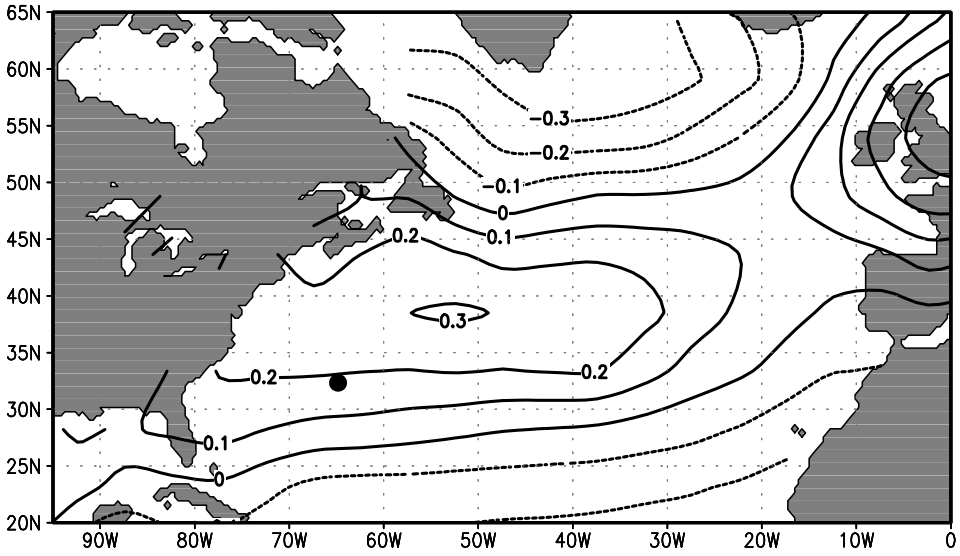

Figure 1. Correlation between annual SSTs and December to February (DJF) NAO index (1860–1991). The dot indicates Bermuda.

variations of local SSTs, only some of them show consistent SST signals at decadal timescales.

[4] In addition to the direct comparisons of proxy and single instrumental time series outlined above some studies include reconstructions of large-scale climatic patterns by means of one or a couple of corals from different drill sites. *Evans et al.* [2002] used empirical orthogonal functions of corals from 12 sites of the tropical oceans in order to reconstruct the first modes of the Pacific SST. Furthermore, field correlations of proxy data with SST or sea level pressure (SLP) are applied in order to detect large-scale climate patterns including El Niño/Southern Oscillation (ENSO) and the North Atlantic Oscillation (NAO) [*Evans et al.*, 1999; *Pfeiffer et al.*, 2004; *Rimbu et al.*, 2001; *Kuhnert et al.*, 2005].

[5] Field correlations directly provide spatial information with the proxy. Thus they are often even better suited to detect climate patterns than correlations with predefined indices or pattern time series, especially if such correlation patterns do not represent a dominant climate pattern (e.g., AO, ENSO). However, a validation of such local coral-based reconstructions of large-scale SST and SLP fields has not been attempted so far.

[6] This is the aim of this work. Validated statistical models will be established for the prediction of large-scale SST and SLP fields from local coral records. This involves the question, as to what extent the local coral records are related to large-scale SST and SLP fields. Secondly a validation check with independent data supplies an assessment for the reliability of the reconstructed patterns. Such so-called upscaling models try to statistically invert the physical processes that determine the proxy, here the coral growth. In cases where several processes influence the proxy, the statistical inference is problematic. This is a limitation of upscaling models compared with, e.g., downscaling models which are capable to regard multiple predictors that are linked to the proxy [*Crüger et al.*, 2004].

[7] Bermuda is of major interest concerning the dominant mode of northern hemispheric climate variability, the AO and NAO, respectively. *Wallace et al.* [1990] found that the first EOF of the North Atlantic SST pattern, which is associated with positive anomalies in Bermuda, is related to a 500 hPa geopotential pattern that resembles the 500 hPa NAO pattern. Further investigations concerning the relationship between North Atlantic SSTs and northern hemispheric SLP show that the winter NAO is positively correlated with the SSTs in Bermuda and the Sargasso Sea, where the maximum correlation is found when SST lags the NAO index by 0–2 years [*Visbeck et al.*, 2003; *Walter and Graf*, 2002]. Investigations with corals showed that temperature records from Bermuda are also strongly influenced by the AO/NAO [*Kuhnert et al.*, 2002; *Cohen et al.*, 2004; *Kuhnert et al.*, 2005]. Figure 1 shows the correlation map of the winter NAO (DJF) and the annual SST (see below) for lag = 0 for the period of 1860–1991. It is characterized by a pronounced pattern of positive correlation values around Bermuda, especially northeast of Bermuda and the North Sea. Negative values are found west of Africa and between Newfoundland and Island. Thus Bermuda can be viewed as a relevant location for the North Atlantic and European climate that makes it reasonable to undertake an upscaling on the basis of proxies from this location.

[8] The aim of our study is to establish validated upscaling models, i.e., statistical regression models for the reconstruction of large-scale climatic patterns from local proxy, here coral records. We use two annual growth records of 140 years length from different coral species (*Diploria strigosa*, *Montastraea cavernosa*) from Bermuda. The *Montastraea* record was taken from the work of *Pätzold et al.* [1999]. A shorter portion (1928–1982) of the *Diploria* material was previously investigated for Sr/Ca by *Kuhnert et al.* [2005], who found a statistically significant correlation of late-year Sr/Ca with the NAO index as well as for subsurface temperatures. The two annual growth records enable us to calibrate and validate transfer functions with the time series of SST and SLP patterns for a relatively long period (140 and 80 years, respectively). Furthermore, we

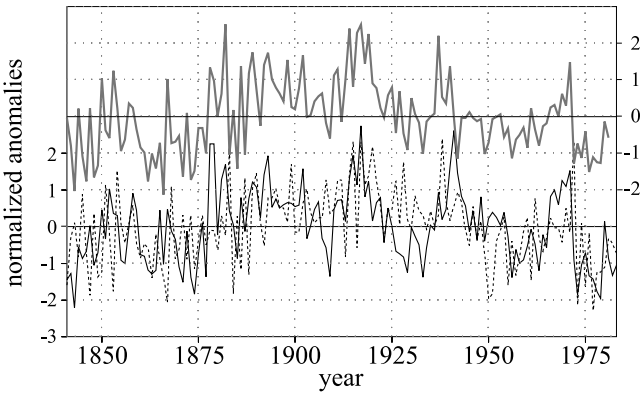

Figure 2. Normalized annual growth rates of DS (dashed curve) and MC (solid curve) and their PC1 (top).

can evaluate, whether corals from adjacent sampling sites represent consistent climate signals, and whether a combination of both records strengthens the climate signals. The paper is structured as follows: After describing the data used, we perform a correlation analysis between the coral time series and the SST and SLP fields. The description of the statistical technique for the development and validation of upscaling models is followed by the presentation of the models for the reconstruction of SST and SLP patterns. Finally, the results will be discussed.

2. Data

2.1. Corals

[9] Two different coral species are used (*Diploria strigosa* and *Montastraea cavernosa*, referred to as DS and MC, respectively). The colonies were recovered from 12 m water depth at the North-East Breakers of Bermuda. Bermuda is influenced by the recirculation of the subtropical gyre. The gyre advects Subtropical Mode Water, which forms south of the Gulf Stream, to Bermuda [*Talley and Raymer*, 1982; *Klein and Hogg*, 1996]. Both sample sites are near the northern margin of the Bermuda reef, where the water masses are well mixed. Therefore we assume that both corals are subjected to the same environmental influences and neglect all local disturbances. Sample preparation followed the standard procedures. Slabs (6 mm thick) were cut parallel to the major growth axis and X-rayed to reveal the density banding pattern. Both corals were similarly analyzed in such way that the middle of each high-density band was chosen to separate two adjacent annual growth increments. High-density bands in our corals formed in late summer to fall.

[10] Thus a growth year in our coral chronology begins and ends approximately with the onset of fall or within early fall. In our study we use the coral data from 1841 until 1983, which comprises the entire DS record and it also represents the period where both records overlap. For both colonies, the investigated section is about 50 cm long. The average annual skeletal extension is about 3.5 mm, which falls within the typical range for massive species in locations exposed to the open ocean at Bermuda [*Dodge*, 1978; *Logan et al.*, 1994].

[11] Figure 2 shows the normalized growth rates from 1841 until 1983 and their leading principal component (PC1). The first empirical orthogonal function (EOF) explains 71% of the coral growth rate variability. Since we normalized the records, both contribute with the same weight to the EOF. The loading of the first EOF is 0.84. This value also represents the correlation between the single coral records with PC1. The mean of the squared correlation coefficients is the explained variance of the EOF (71%). The correlation between both coral records is 0.45 for the entire period from 1841 until 1983, after the trend is removed.

2.2. Instrumental Data

2.2.1. Sea Surface Temperatures (SSTs)

[12] The SSTs used in this work are derived from the monthly anomalies of the MOHSST5 data set based on the GOSTA data set of the U.K. Meteorological office [*Parker et al.*, 1994; *Kaplan et al.*, 1998]. The period covered by this data set is from 1856 until 1991. Because of the statistical procedures that utilizes available observations at all space points and information from all times [*Hurrell and Trenberth*, 1999], the data set has no missing values on a 5×5 grid. A detailed description of the statistical method is found in work by *Kaplan et al.* [1997, 1998]. The anomalies of the SSTs are based on the 1951–1980 time period. For our purpose, we calculated the annual mean anomalies. Seasonal means were also tested, but they did not yield better results. For the assessment of correlation values calculated with these SSTs we tested the 1-year lag autocorrelation of the SSTs. Around Bermuda correlation values of at least 0.4, north of Bermuda even 0.5 are obtained, leading to a considerable reduction of the degrees of freedom of the SST time series and consequently to an increase of the significance thresholds for correlation values obtained with these data (not shown). For 1-year lag autocorrelation values of, e.g., 0.5, the degrees of freedom decrease to about one third of the total time series length [*Leith*, 1973].

2.2.2. Sea Level Pressure (SLP)

[13] The SLP data set provided by NCAR is used, which is described in detail by *Trenberth and Paolino* [1980]. The period of this data set is from 1899 until 1983. It covers nearly the entire Northern Hemisphere from 20 N to the pole, however, with occasionally missing values at high latitudes and in Asia. From the monthly values, the winter mean for the December to February (DJF) months are calculated yielding the strongest signal with the coral records. Lag-1 correlation of DJF SLP is clearly smaller than for the SSTs and can be neglected over the areas considered here (not shown).

3. Results

3.1. Correlation Maps

3.1.1. Growth Rates and SSTs

[14] Generally, growth rates are found to be positively correlated with local SSTs [*Bessat and Buigues*, 2001; *Lough and Barnes*, 1997; *Slowey and Crowley*, 1995; *Carricart-Ganivet*, 2004]. This is in contrast to Bermuda corals, for which the correlation values between the annual growth rates and the local gridded annual SST are -0.4 for DS, -0.38 for MC and -0.45 for PC1. Bermuda is located in the northwestern part of the Sargasso Sea and accom-

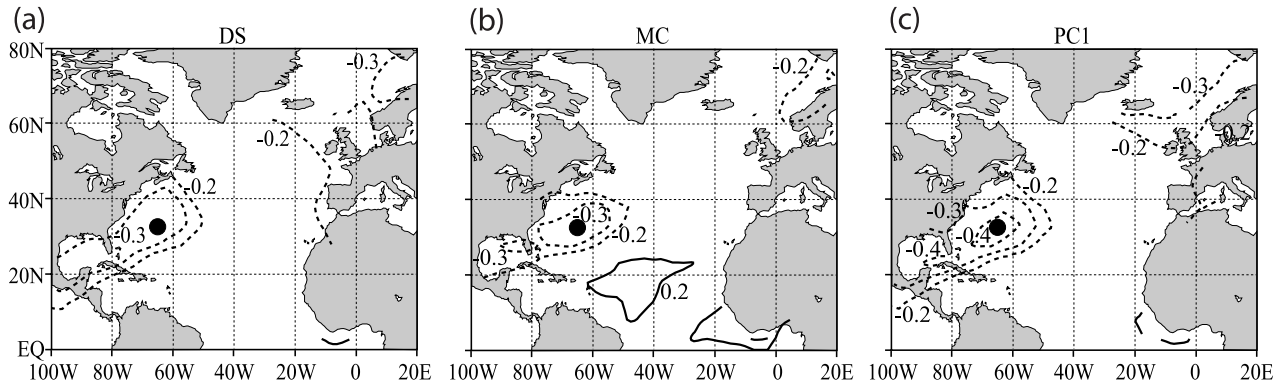

Figure 3. Correlation between annual SSTs (September to August) and coral growth rates (1857–1981): (a) DS, (b) MC, and (c) PC1.

modates the northernmost subtropical coral reefs in the Atlantic Ocean. In contrast to many other reefs, annual skeletal extension in Bermuda corals is significantly but negatively correlated with SST [*Dodge and Vaišnys*, 1975; *Logan et al.*, 1994; *Pätzold*, 1994]. This relationship is indirect: in years with cooler water temperatures vertical mixing is more intense [*Bates*, 2001], which leads to an increase in nutrient supply (and consequently in plankton) in the surface water.

[15] In Figure 3 the correlation maps are shown for the North Atlantic SSTs with the two single corals and their PC1, respectively. All time series were previously detrended. Only values of magnitude higher than 0.2 are displayed. Since around Bermuda the 1-year lag autocorrelation for SSTs is from about 0.4 up to more than 0.5 (see above), the number of degrees of freedom decreases to about 45 in this area [*Leith*, 1973]. Therefore only correlations with magnitude higher than about 0.3 are statistically significant at the 95% level. The correlation maps for the single coral records show that there are negative values around Bermuda up to the US coast and the Gulf of Mexico, which partly reach significance (95%) (Figures 3a and 3b). The highest values are found for PC1 with amounts higher than 0.4 around Bermuda and in the Gulf of Mexico. Therefore the area with statistically significant values has also been increased using PC1, strengthening the SST signal (Figure 3c).

3.1.2. Growth Rates and SLP Fields

[16] For Bermuda, the correlation between SLP and coral growth was noted by *Dodge and Vaišnys* [1975], who attributed this to increased light levels that are concurrent with high SLP. Whereas the highest correlation between the corals and the SSTs is found for simultaneous time series, the correlation between coral growth rates and SLP is highest when the growth records lag the SLP by one year.

[17] Figure 4 shows the correlation maps for the single corals (Figures 4a and 4b) and for PC1 of the coral records (Figure 4c) (scaled by −1) between 1901 and 1983. All patterns show negative values over the polar region, whereas over the North Atlantic and the North Pacific positive values occur. This structure is strongest for DS. The highest correlation values are found in these regions, which are statistically significant over large areas of the Northern Hemisphere. This pattern clearly resembles the pattern of the AO [*Thompson and Wallace*, 1998] and the NAO, respectively [*Jones et al.*, 1997]. The correlation between DS and the AO index is $r = -0.43$. Smaller, but also statistically significant (at the 95% level), is the correlation

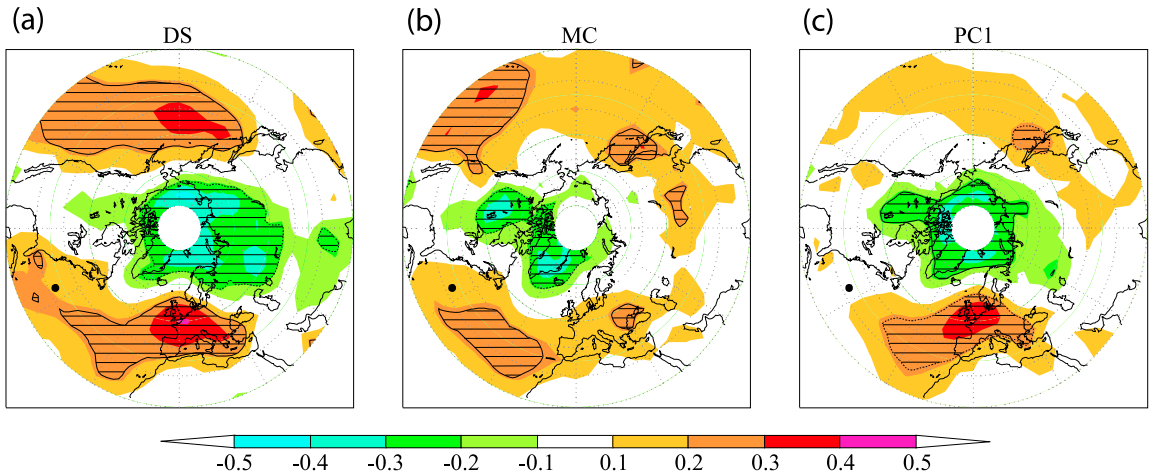

Figure 4. Correlation between SLP (DJF) and coral growth rates (1901–1981; SLP leads coral by one year): (a) DS, (b) MC, and (c) PC1 (scaled by −1; statistically significant values are indicated by the hatched areas).

value between DS and the NAO index, for which $r = -0.26$ is found. For MC and PC1, however, the correlation values are not as high as for DS and the patterns only weakly resemble the AO pattern. This is also reflected by the correlation values with the AO index, which is -0.29 for MC and -0.19 for PC1. Thus, in contrast to the SSTs, the clearest signal in the SLP is found for one single coral record.

3.2. Upscaling Models

[18] We have shown that the single coral time series and/or PC1 of both series yield statistically significant correlation values with large-scale SSTs and wide parts of hemispheric SLP fields. However, does this also mean that we can reliably reconstruct past SST or SLP patterns? In order to investigate this question, we developed upscaling models; that is, we calibrated large-scale SST and SLP pattern time series against local coral time series. We apply a simple regression method; that is, we directly relate the proxy to the local climatic parameter field, resulting in a regression map, which is accompanied with the proxy. This map is the basis for calibration. Another method would be to calculate the EOFs of the climatic field and use the principal components for calibration. In this case, a reduction of degrees of freedom is achieved, however, the patterns are independently derived from the proxies. A reconstruction is then achieved by a linear combination of the principal components [*Evans et al.*, 2002; *Crüger et al.*, 2004].

3.2.1. Statistical Technique

[19] The regression models presented in this work consist of regression patterns between local coral time series and the SLP/SST time series field:

$$f_{SLP/SST}(x) = r(x)\frac{s_{SLP/SST}(x)}{s_{coral}} \quad (1)$$

Here, $f_{SLP/SST}(x)$ denotes the regression coefficient for an estimation of $SLP/SST(x, t)$, $r(x)$ the correlation coefficient and $s_{SLP/SST}(x)$ and s_{coral} the standard deviations of the climatic fields and the corals, respectively. A reconstruction of $SLP/SST(x, t)$ can be obtained by multiplying the regression map $f_{SLP/SST}(x)$ with the coral time series $c(t)$. Besides the structure of the regression pattern, the regression model is essentially defined by the spatial extent of the *SLP/SST* regression map.

[20] In detail, the following steps are performed for calibration:

[21] 1. We calculate a regression map $f_{SLP/SST}(x)$ with detrended anomalies for a reconstruction of a SLP/SST time series.

[22] 2. We visually assess and select an area, where the coral record is suggested to represent the SLP/SST. Here we looked for considerable regression coefficients and/or pronounced structures.

[23] 3. We reconstruct the SLP/SST projection index time series $F_{SLP/SST}(t)$ from the projection of the regression map $f_{SLP/SST}(x)$ onto the SLP/SST anomalies $A_{SLP/SST}(x, t)$, minimizing e(t):

$$A_{SLP/SST}(x,t) = F_{SLP/SST}(t) f_{SLP/SST}(x) + e(t) \quad (2)$$

[24] 4. We calculate the variance of the projection index time series $F_{SLP/SST}(t)$ that is explained by the coral time series $c(t)$.

[25] 5. We vary the spatial boundaries of the regression map and repeat step 3 and 4 in order to maximize the explained variance.

[26] In order to get a statistically reliable regression model, we verified the regression models with data which has not been used for calibration. This is carried out with the cross-validation technique [*Michaelsen*, 1987; *von Storch and Zwiers*, 1999], which has been used before for other paleoclimate reconstructions [*Crüger et al.*, 2004; *Crüger and von Storch*, 2002; *Glueck and Stockton*, 2001; *Jones and Widmann*, 2003]. In this procedure the available data are divided into calibration and validation data. The calibration data are used for the calculation of the regression map which in turn is the basis for the reconstruction of the SLP/SST index time series for the validation time step. Performing this procedure stepwise for every time step, all time steps are eventually used for validation.

[27] The following steps are performed for validation:

[28] 1. We separate data into calibration and validation data.

[29] 2. We calculate the regression map obtained from the detrended calibration data.

[30] 3. We estimate $F_{SLP/SST}(t = t_{val})$ for the validation time step t_{tval}. Note that the SLP/SST anomaly $A_{SLP/SST}(x, tval)$ for the validation time step is related to the mean of the calibration period.

[31] 4. We stepwise repeat steps 1–3 until all time step indices are reconstructed.

[32] 5. We calculate the variance of the projection index time series explained by the coral time series.

[33] A prediction of the SST/SLP field is obtained performing the following steps:

[34] 1. We calculate the proxy anomalies related to the mean of the calibration period.

[35] 2. We multiply the regression pattern obtained using equation (1) with the anomaly of the proxy. This yields a SST/SLP anomaly field time series.

[36] Upscaling models were developed for the SST as well as the SLP fields. In order to guarantee that the data of the validation time step is completely independent of the model calibration data [*von Storch and Zwiers*, 1999], we removed 11 time steps from the calibration period for the SLP model. For the SST model we dropped 21 time steps, because of the high autocorrelation of the SST data. For the SLP model the 6th and for the SST model the 11th time step of the removed steps was used for validation.

[37] In order to find out which of the three coral records yields the best estimate, we established upscaling models for the single coral records as well as for their PC1. Furthermore, we checked whether the use of smoothed data improves the results.

3.2.2. Upscaling Model for SST Fields

[38] For the SST, satisfactory results are only obtained using data smoothed with a 5-year running mean. That is, only multiannual variability is described by the regression models. The highest explained variance is obtained for PC1 of the corals. This model explains about 30% of the variance of the smoothed, i.e., the multiannual SST field. For the single coral records only 27.5% (MC) and 20% (DS)

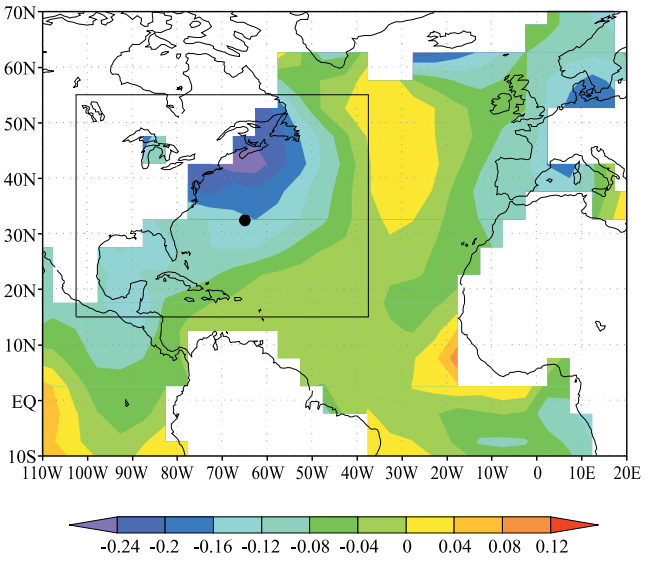

Figure 5. Regression pattern between annual SST (September–August) and PC1 1857–1981 (K) (data smoothed with a 5-year running mean).

could be achieved. Note that the smoothing procedure reduces the variance of the SST field. For the area of the regression model the total amount of variance is reduced by around 50%. Thus the regression model based on PC1 explains 15% of the original SST field variability. For all of these three upscaling models the spatial extensions of the regression patterns are the same. This indicates that each coral record actually represents the SSTs of the same area, however, with a different amount of explained variance.

[39] In the following, we only refer to the best upscaling model, i.e., the model based on PC1. Figure 5 shows the regression pattern for the North Atlantic. The square denotes the area of the model. The boundaries of the regression map range from Newfoundland in the north to the Caribbean Sea in the south and the Gulf of Mexico in the west to 40°W in the middle Atlantic. The pattern is characterized by high negative regression values north of Bermuda with a strong gradient reaching regression values around zero near the eastern and southern boundaries. Differences between the regression and the correlation map (Figure 3c) occur because the regression coefficient involves the spatially varying standard deviation of the SST (equation (1)). It gets the highest values north of Bermuda (not shown), which is reflected in the regression map.

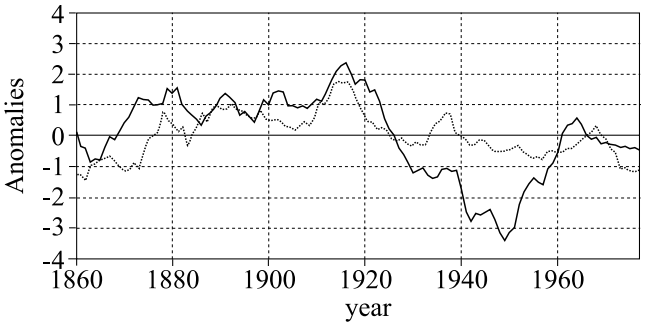

Figure 6. PC1 (dotted curve) and cross-validated SST time series (solid curve) of SST upscaling model.

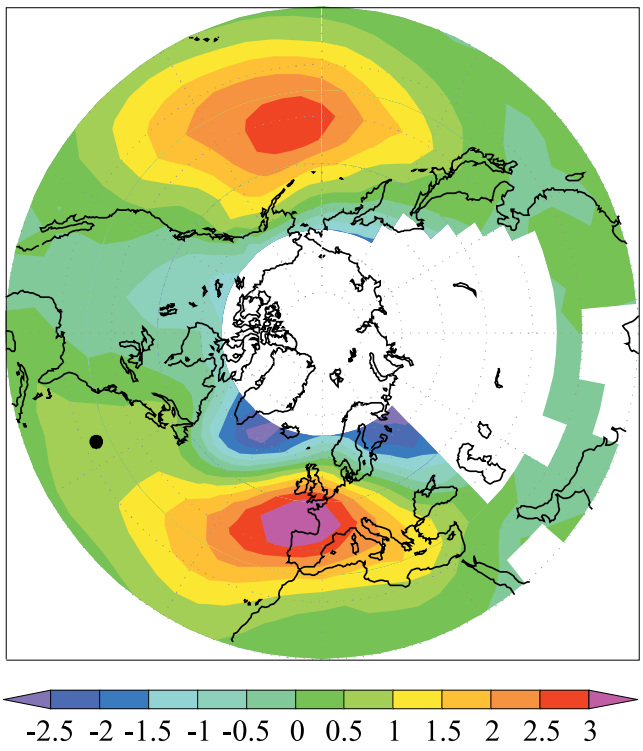

Figure 7. Regression between SLP (DJF) and DS (hPa yr/mm), (scaled by −1; SLP leads coral by 1 year).

[40] Figure 6 shows the time series that corresponds with the regression pattern and the coral time series. Until about 1930 both curves match relatively well. From 1930 until about 1960, however, the SST projection indices have much higher amounts compared with PC1.

3.2.3. Upscaling Model for SLP Fields

[41] For the SLP, the upscaling models yield the best results when the raw data are used, without smoothing procedure. Using smoothed data worsens the results markedly. As it can be expected from the correlation maps, the best upscaling model for the SLP is obtained for DS when the SLP leads the coral time series by one year.

[42] We only show the results for DS. The regression map is shown in Figure 7. The white areas of the map denote the areas where there are missing SLP values in some years. Therefore we disregarded these areas for our regression. In Figure 8 the validated time series are shown. The trends of

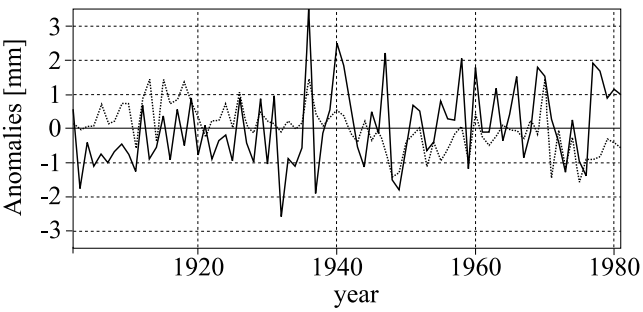

Figure 8. DS annual growth rates (dotted curve) and cross-validated SLP time series (solid curve) of SLP upscaling model.

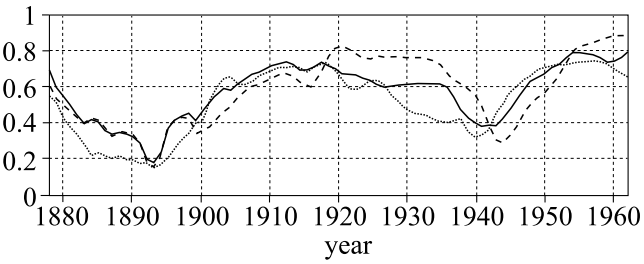

Figure 9. Running correlation between Bermuda SST (4 grid points) and coral time series: DS (dotted curve), MC (dashed curve), and PC1 (solid curve). All data are smoothed with a 5-year running mean, window width 40 years (scaled by −1).

both curves do not agree and have opposite direction. When the trends are removed, the explained variance is 21%. The interannual variations are well reproduced. This means that the coral describes interannual variations of the SLP pattern, but no long-term trends. Furthermore, multiannual variations are not reproduced by the model either, since a model based on smoothed data yields worse results.

4. Discussion

[43] We have shown that the growth rates of two different colonies of corals from Bermuda represent overall similar climate signals, confirming that reconstructing climate patterns from single coral records is basically a valid approach. Both coral records have similar correlation maps with annual SSTs, showing negative values from the northern parts of the Sargasso Sea up to Nova Scotia in the north and the Gulf of Mexico in the west. The SST signal is strongest when using PC1 of the corals. In contrast to the SST, the SLP signal is strongest for one coral (DS), when the SLP leads the coral by one year. This coral shows a hemispheric SLP signal that is clearly related to the AO pattern, which is also evident for MC, but less pronounced.

[44] In order to ascertain whether the partly statistically significant correlation values are a sufficient condition to reliably reconstruct the amplitudes of SST and SLP patterns, respectively, we established upscaling models which were checked by cross validation. The best validation results are obtained for the coral time series that shows the highest correlation values with SST or SLP time series, a result that was also inferred from the correlation maps. PC1 describes best a SST pattern that covers the western part of the North Atlantic, from the Caribbean Sea up to Newfoundland. These extensions also denote the area for which the SSTs are represented by the corals. Substantially enlarging the areas worsens the validation results.

[45] About 30% of the multiannual SST field is explained by the smoothed coral growth rate PC1. Using raw data reduces the explained variance. The model for the SLP field is based on only one single coral (DS). Interannual SLP pattern variations can be reconstructed; trends are not described by the statistical model. 21% of the SLP variance is expressed in the coral record, after the trends of DS and the SLP pattern time series are removed. Using smoothed data for the SLP regression model markedly decreases the explained variance. This has been expected, since the NAO is mainly determined by high-frequency variability, which is widely canceled out by smoothing over several years.

[46] The explained variance of 21% corresponds to a correlation coefficient of 0.45, which is more than any local correlation coefficient between SLP and DS (Figure 4a). However, one should keep in mind that the increased correlation refers to the index time series of the regression pattern which explains only a proportion of the real SLP time series field. The main deficiency of the upscaling models is the failure to estimate linear trends. This has also been found by *Lough* [2004] for some of her investigated coral δ^{18}O time series.

[47] In order to further evaluate our results, especially with respect to the analysis of both corals, we repeated our computations for different lags and periods. We found that for a lag of zero and 2 years (SLP leads the coral record by 2 years) the signal for both corals is substantially reduced. On the other hand, when calculating the correlation with SST for the period investigated for the SLP (1900 until 1983) with a lag of one year, the maps for both corals remain similar.

[48] Additionally we performed running correlations with the unsmoothed coral time series. This results in correlation coefficients of about 0.4 until 1940 increasing up to 0.5 later on. We assume that it is unlikely that our results are compromised by dating errors. The density banding pattern of both corals is very clear, with the exception of the youngest few years in MC. There is no indication of growth hiatuses or multiple band couplets in a year. Nevertheless we performed tests with removing and adding one annual band, which did not substantially change or even improve the results. Therefore we exclude that a shift in parts or the entire record is responsible for the weaker SLP signal of MC.

[49] However, it is possible that the response of the corals to climate signals vary in time. We verified this by the running correlation values between the mean of four SSTs grid points next to the sampling site and the three coral time series (Figure 9). Since the upscaling model for SSTs is based on smoothed data, we also used smoothed data for these calculations. The window width is 40 years. Figure 9 reveals that the correlation values obtained for both corals widely agree. Thus we exclude that the analysis of the corals are stochastically dominated, as could be suspected from *Gershunov et al.* [2001], despite we are aware of the high autocorrelation of the smoothed data. Figure 9 shows that the correlation values are not stable in time, but vary between negative values of amount more than 0.8 and values just reaching 0.2. This suggests that the corals are only indirectly related to SST, leading to a temporally unstable relationship with local SST. Thus we assume that the relationship between SST and those parameters that are directly related to coral growth, probable nutrients, is not stable in time.

[50] Bermuda corals have been previously found to record the AO/NAO variability in their skeletal chemistry [*Cohen et al.*, 2004; *Kuhnert et al.*, 2005]. We have shown that similar relationships exist between large-scale SLP, regional SST and local growth rates. However, our results reveal different response times of the corals to variations of SST and SLP, respectively: Whereas the corals and SSTs are synchronously linked, the corals lag SLP variations by one

year. In order to evaluate this, we calculated the correlation map between the North Atlantic SSTs and the AO index. The pattern widely corresponds with that between PC1 and SST (Figure 3c), when there is no lag between the series. However, only a weak signal is found, when the AO leads the SST by one year.

[51] Furthermore, we calculated the correlation between the DJF SLP and the regional Bermuda SST for the data used here. The map for lag = 0 shows a similar pattern as those between the corals and DJF SLP (Figure 4), however, with somewhat smaller correlation values, also confirming the link between the large-scale SLP pattern and regional SSTs.

[52] These results are obtained with lag = 0 in contrast with those found with the coral records, where SLP leads by one year. We suggest that this discrepancy is a result of a shift of the signals for a couple of months, which is not resolved in the annual values used in this work. We suppose that the 'true' lag between SLP and SST and that of SLP and coral growth is within 0 to 12 months. Former works also revealed considerable correlations between the North Atlantic SST and NAO at lags between 0 and 2 years. Thus our results are within this range [*Visbeck et al.*, 2003; *Walter and Graf*, 2002] (see also Figure 1).

[53] It has been suggested earlier that Bermuda corals are only indirectly related to SST [*Dodge and Vaišnys*, 1975]: Coral growth is essentially driven by the supply of nutrients, which are brought from deeper layers to the surface. This is accompanied by decreasing temperatures in the upper layer, leading to a negative correlation between SST and coral growth.

[54] This hypothesis is confirmed by *Oschlies* [2001], who investigated the influence of the NAO to the nutrient supply in the surface waters of the North Atlantic with a coupled ecosystem-circulation model. Around Bermuda he found a decrease of nutrients in the euphotic zone of about 30% between the NAO-low and NAO-high experiment. This decrease is mainly attributed to the shallower vertical mixing in the NAO-high experiment. Furthermore he evaluated that upwelling has only little influence. This is in line with *Marshall et al.* [2001], who evaluated for the North Atlantic the wind stress curl, which is a measure upwelling. Whereas the mean of the wind stress curl shows a minimum (i.e., anticyclonic circulation) over Bermuda, zero wind stress curl is obtained for NAO(+) conditions. This suggests that NAO-induced upwelling does not substantially influence the nutrients' supply in Bermuda.

[55] The regression model for the reconstruction of the SLP field is based on only one coral, whereas that for the reconstruction of the SST field is based on PC1. Primarily we expected the best results for the combined coral series for the SLP as well as for the SST field, since we assumed to reduce the noise proportion from the combined series. However, our results suggest that at least for the SLP, DS represents a larger proportion than MC, which leads to worse results for PC1 than for DS, despite the assumed higher noise proportion in DS.

[56] Is it possible that one species is more appropriate to record a specific climate parameter, whereas another species better archive a second parameter, although both corals are subjected to the same environmental influences? Natural variability within one species as well as differences in the microenvironment can lead to small differences in the records between neighboring colonies. While this may explain intercolony variability on short timescales, it is unlikely to result in differences on the multiyear scale, and it does not explain differences in the sensitivities to changes in SLP and SST as observed in our records. It is interesting to note that the autocorrelation of the used corals are markedly different, for DS 0.12 and for MC 0.54. From this one could speculate that both corals actually archive slightly different climate signals, namely that DS better describes SLP, both having a white spectrum, whereas MC describes better SST, whose spectra are red. We suggest that species-specific sensitivity to environmental variability plays an important role. For example, results from Caribbean corals of the same genera (but different species) used here suggest that skeletal extension in *M. annularis* is stronger influenced by changes in nutrient levels than *D. labyrinthiformis*, where light (cloudiness) seems to be more important [*Charry et al.*, 2004].

[57] It is important to note that apart from the above mentioned factors coral skeletal extension is potentially influenced by a broad range of variables. These include, for example, wave energy, sedimentation and turbidity [*Dodge et al.*, 1974; *Dodge*, 1982; *Logan et al.*, 1994]. It is therefore difficult to explain the statistical relationships between growth rates and SST and SLP on a physical basis, because the coral actually responds to a whole array of environmental variables that may or may not act in concert.

[58] In any case these autocorrelations confirm our results that SLP is better described by DS. A combined series of MC and DS, the latter has negligible autocorrelation, describes SST better. The autocorrelation of these combined series has been artificially increased by smoothing in order for a better description of the SST, which has high autocorrelation in contrast to SLP.

5. Conclusions

[59] We have shown that the proxy records from two coral species from Bermuda on the whole show similar SST and SLP signals, leading to an increased confidence of climate signals detected in coral records.

[60] Upscaling models for large-scale SST and SLP patterns have been developed, which explain 30% of the multiannual (SST) and 21% of the interannual detrended (SLP) variability of the pattern time series after validation. Problems remain in reconstructing long-term trends. Thus, even if proxy data are statistically significantly correlated with climate parameters in a certain period, they are not necessarily suitable to reliably reconstruct the linear trends of past climates.

[61] The upscaling model for the SST field is based on PC1 of both corals and for the SLP on one coral (DS). Therefore we conclude that utilizing several corals potentially improve the reconstructions of climate pattern time series. This has to be proven for each proxy and each predictand to be reconstructed. On the other hand our results suggest that different coral species archive climate signals to a slightly different degree. This indicates that it is reasonable to construct a master chronology with corals of the same species.

[62] Our method evaluates the areas, whose SST/SLP is represented by the local coral record. Furthermore, the reconstruction skill of different proxies can be proved by our method. Thus our method can help to find optimal proxies for climatic reconstructions in local or regional scale, which has also been attempted by *Pauling et al.* [2003]. An extension of our technique, utilizing multiple proxies from well separated sites could be applied for a reconstruction of climatic parameters for multiple areas adding them up to global scale.

[63] In our study we have used coral growth rates to demonstrate the potential of upscaling models for reconstructing large-scale climate patterns from local proxy time series. This technique yields more spatial information than the reconstruction of climate indices alone. Upscaling models can easily be applied to other proxy archives as well, for example, ice cores, speleothems, and tree rings. Future studies incorporating the latter would be particularly interesting. Since tree ring data are usually based on a large number of parallel time series, upscaling models could be used to identify the best subset for reconstructing climate patterns, which in turn would help to optimize the strategy for sample collection.

[64] **Acknowledgments.** Kaplan SST data were provided by the NOAA-CIRES Climate Diagnostics Center, Boulder, Colorado, United States, from their Web site at http:/www.cdc.noaa.gov. This study was supported through BMBF grant 01LD0031 (DEKLIM). H.K. was partially funded by the DFG Research Center for Ocean Margins (RCOM0408). We are grateful to the anonymous reviewers for their helpful comments.

References

Alibert, C., and M. T. McCulloch (1997), Strontum/calcium records in modern Porites corals from the Great Barrier Reef as a proxy for sea surface temperature: Calibration of the thermometer and monitoring of ENSO, *Paleoceanography*, *1*, 345–363.

Bates, N. R. (2001), Interannual variability of oceanic CO_2 and biogeochemical properties in the western North Atlantic subtropical gyre, *Deep Sea Res., Part II*, *48*, 1507–1528.

Bessat, F., and D. Buigues (2001), Two centuries of variation in coral growth in a massive Porites colony from Moorea (French Polynesia): A response of ocean-atmosphere variability from south central Pacific, *Palaeogeogr. Palaeoclimatol. Palaeoecol.*, *175*, 381–392.

Carricart-Ganivet, J. P. (2004), Sea surface temperature and the growth of the west Atlantic reef-building coral *Montastrea annularis*, *J. Exp. Mar. Biol. Ecol.*, *302*, 249–260.

Charry, H., E. M. Alvarado, and J. A. Sánchez (2004), Annual skeletal extension of two reef-building corals from the Colombian Caribbean Sea, *Bol. Invest. Mar. Cost.*, *33*, 209–222.

Cobb, K. M., C. D. Charles, H. Cheng, and R. L. Edwards (2003), El Nino/Southern Oscillation and tropical Pacific climate during the last millennium, *Nature*, *424*, 271–276.

Cohen, A. L., S. R. Smith, M. S. McCartney, and J. van Etten (2004), How brain corals record climate: An integration of skeletal structure, growth and chemistry of *Diploria labyrinthiformis* from Bermuda, *Mar. Ecol. Prog. Ser.*, *271*, 147–158.

Cole, J. E., and R. G. Fairbanks (1990), The Southern Oscillation recorded in the $\delta^{18}O$ of corals from Tarawa Atoll, *Paleoceanography*, *5*, 669–683.

Crowley, T. J., T. M. Quinn, and W. T. Hyde (1999), Validation of coral temperature calibrations, *Paleoceanography*, *14*, 605–615.

Crüger, T., and H. von Storch (2002), Creation of "artificial ice core" accumulation from large-scale GCM data: Description of the downscaling method and application to one north Greenland ice core, *Clim. Res.*, *20*, 141–151.

Crüger, T., H. Fischer, and H. von Storch (2004), What do accumulation records of single ice cores in Greenland represent?, *J. Geophys. Res.*, *109*, D21110, doi:10.1029/2004JD005014.

Dodge, R. E. (1978), The natural growth records of reef building corals, Ph.D. thesis, Yale Univ., New Haven, Conn.

Dodge, R. E. (1982), Effects of drilling mud on the reef-building coral *Montastrea annularis*, *Mar. Biol.*, *71*, 141–147.

Dodge, R. E., and J. R. Vaišnys (1975), Hermatypic coral growth banding as environmental recorder, *Nature*, *258*, 706–708.

Dodge, R. E., R. C. Aller, and J. Thomson (1974), Coral growth related to resuspension of bottom sediments, *Nature*, *247*, 574–577.

Evans, M. N., R. G. Fairbanks, and R. L. Rubenstone (1999), The thermal oceanographic signal of El Niño reconstructed from a Kiritimati Island coral, *J. Geophys. Res.*, *104*, 13,409–13,421.

Evans, M. N., A. Kaplan, and M. A. Cane (2002), Pacific sea surface temperature field reconstructions from coral $\delta^{18}O$ data using reduced space objective analysis, *Paleoceanography*, *17*(1), 1007, doi:10.1029/2000PA000590.

Felis, T., J. Pätzold, Y. Loya, M. Fine, A. H. Nawar, and G. Wefer (2000), A coral oxygen isotope record from the northern Red Sea documenting NAO, ENSO, and North Pacific teleconnections on the Middle East climate variability since the year 1750, *Paleoceanography*, *15*, 679–694.

Felis, T., G. Lohmann, H. Kuhnert, S. J. Lorenz, D. Scholz, J. Pätzold, S. A. Al-Rousan, and S. Al-Moghrabi (2004), Increased seasonality in Middle East temperatures during the last interglacial period, *Nature*, *429*, 164–168.

Gagan, M. K., L. K. Ayliffe, J. W. Beck, J. E. Cole, E. R. M. Druffel, R. B. Dunbar, and D. P. Schrag (2000), New views of tropical paleoclimates from corals, *Quat. Sci. Rev.*, *19*, 45–64.

Gershunov, A., N. Schneider, and T. Barnett (2001), Low-frequency modulation of the ENSO-Indian monsoon rainfall relationship: Signal or noise?, *J. Clim.*, *14*, 2486–2492.

Glueck, M. F., and C. W. Stockton (2001), Reconstruction of the North Atlantic Oscillation, *Int. J. Climatol.*, *21*, 1453–1465.

Hurrell, J. W., and K. E. Trenberth (1999), Global sea surface temperature analysis: Multiple problems and their implications for climate analysis, modeling, and reanalysis, *Bull. Am. Meteorol. Soc.*, *80*, 2661–2678.

Jones, J. M., and M. Widmann (2003), Instrument- and tree-ring-based estimates of the Antarctic Oscillation, *J. Clim.*, *16*, 3511–3524.

Jones, P. D., T. Jonsson, and D. Wheeler (1997), Extension to the North-Atlantic Oscillation using early instrumental pressure observations from Gibraltar and south-west Iceland, *Int. J. Climatol.*, *17*, 1433–1450.

Kaplan, A., Y. Kushnir, M. A. Cane, and M. B. Blumenthal (1997), Reduced space optimal analysis for historical data sets: 136 years of Atlantic sea surface temperatures, *J. Geophys. Res.*, *102*, 27,835–27,860.

Kaplan, A., M. A. Cane, Y. Kushnir, A. C. Clement, M. B. Blumenthal, and B. Rajagopalan (1998), Analyses of global sea surface temperature 1856–1991, *J. Geophys. Res.*, *103*, 18,567–18,589.

Klein, B., and N. Hogg (1996), On the variability of 18 degree water formation as observed from moored instruments at 55°W, *Deep Sea Res., Part I*, *43*, 1777–1806.

Kuhnert, H., J. Pätzold, B. G. Hatcher, K.-H. Wyrwoll, A. Eisenhauer, L. B. Collins, Z. R. Zhu, and G. Wefer (1999), A 200-year coral stable oxygen isotope record from a high-latitude reef off Western Australia, *Coral Reefs*, *18*, 1–12.

Kuhnert, H., J. Pätzold, B. Schnetger, and G. Wefer (2002), Sea-surface temperature variability in the 16th century at Bermuda inferred from coral records, *Palaeogeogr. Palaeoclimatol. Palaeoecol.*, *179*, 159–171.

Kuhnert, H., T. Crüger, and J. Pätzold (2005), NAO signature in Sr/Ca ratios in a Bermuda coral, *Geochem. Geophys. Geosyst.*, *6*, Q04004, doi:10.1029/2004GC000786.

Leith, C. E. (1973), The standard error of time-averaged estimates of climatic means, *J. Appl. Meteorol.*, *21*, 1066–1069.

Linsley, B. K., R. B. Dunbar, G. M. Wellington, and D. A. Mucciarone (1994), A coral-based reconstruction of Intertropical Convergence Zone variability over Central America since 1707, *J. Geophys. Res.*, *99*, 9977–9994.

Linsley, B. K., G. M. Wellington, D. P. Schrag, L. Ren, M. J. Salinger, and A. W. Tudhope (2004), Geochemical evidence from corals for changes in the amplitude and spatial pattern of South Pacific interdecadal climate variability over the last 300 years, *Clim. Dyn.*, *22*, 1–11, doi:10.1007/s00382-003-0364-y.

Logan, A., L. Yang, and T. Tomascik (1994), Linear skeletal extension rates in two species of Diploria from high-latitude reefs in Bermuda, *Coral Reefs*, *13*, 225–230.

Lough, J. M. (2004), A strategy to improve the contribution of coral data to high-resolution paleoclimatology, *Palaeogeogr. Palaeoclimatol. Palaeoecol.*, *204*, 115–143.

Lough, J. M., and D. J. Barnes (1997), Several centuries of variation in skeletal extension, density and calcification in massive Porites colonies from the Great Barrier Reef: A proxy for seawater temperature and a background of variability against which to identify unnatural change, *J. Exp. Mar. Biol. Ecol.*, *211*, 29–67.

Marshall, J., H. Johnson, and J. Goodman (2001), A study of the interaction of the North Atlantic Oscillation with ocean circulation, *J. Clim.*, *14*, 1399–1421.

McConnaughey, T. A. (1989), ^{13}C and ^{18}O isotopic disequilibrium in biological carbonates: I. Patterns, *Geochim. Cosmochim. Acta*, *53*, 151–162.
Michaelsen, J. (1987), Cross-validation in statistical climate forecast models, *J. Clim. Appl. Meteorol.*, *26*, 1589–1600.
Oschlies, A. (2001), NAO-induced long-term changes in nutrient supply to the surface waters of the North Atlantic, *Geophys. Res. Lett.*, *28*, 1751–1754.
Parker, D. E., P. D. Jones, C. K. Folland, and A. Bevan (1994), Interdecadal changes of surface temperature since the late nineteenth century, *J. Geophys. Res.*, *99*, 14,373–14,399.
Pätzold, J. (1984), Growth rhythms recorded in stable isotopes and density bands in the reef coral Porites lobata (Cebu, Philippines), *Coral Reefs*, *3*, 87–90.
Pätzold, J. (1994). Coral proxy records from the Bermudas, paper presented at American Society of Limnology and Oceanography (ASLO) and Phycological Society of America (PSA) Joint Meeting, Miami, Fla.
Pätzold, J., T. Bickert, B. Flemming, H. Grobe, and G. Wefer (1999), Holozänes Klima des Nordatlantiks aus massiven Korallen von Bermuda, *Natur Mus.*, *129*, 165–177.
Pauling, A., J. Luterbacher, and H. Wanner (2003), Evaluation of proxies for European and North Atlantic temperature field reconstructions, *Geophys. Res. Lett.*, *30*(15), 1787, doi:10.1029/2003GL017589.
Pfeiffer, M., O. Timm, W.-C. Dullo, and S. Podlech (2004), Oceanic forcing of interannual and multidecadal climate variability in the southwestern Indian Ocean: Evidence from a 160 year coral isotopic record (La Réunion, 55°E, 21°S), *Paleoceanography*, *19*, PA4006, doi:10.1029/2003PA000964.
Quinn, T. M., and D. E. Sampson (2002), A multiproxy approach to reconstructing sea surface conditions using coral skeleton geochemistry, *Paleoceanography*, *17*(4), 1062, doi:10.1029/2000PA000528.
Rimbu, N., G. Lohmann, T. Felis, and J. Pätzold (2001), Arctic Oscillation signature in a Red Sea coral, *Geophys. Res. Lett.*, *28*, 2959–2962.
Slowey, N. C., and T. J. Crowley (1995), Interdecadal variability of Northern Hemisphere circulation recorded by Gulf of Mexico corals, *Geophys. Res. Lett.*, *22*, 2345–2348.
Smith, S. V., R. W. Buddemeier, R. C. Redalje, and J. E. Houck (1979), Strontium-calcium thermometry in coral skeletons, *Science*, *204*, 404–407.
Talley, L. D., and M. E. Raymer (1982), Eighteen degree water variability, *J. Mar. Res.*, *40*, suppl., 757–775.
Thompson, D. W. J., and J. M. Wallace (1998), The Arctic Oscillation signature in the wintertime geopotential height and temperature fields, *Geophys. Res. Lett.*, *25*, 1297–1300.
Timm, O., M. Pfeiffer, and W.-C. Dullo (2005), Nonstationary ENSO-precipitation teleconnection over the equatorial Indian Ocean documented in a coral from the Chagos Archipelago, *Geophys. Res. Lett.*, *32*, L02701, doi:10.1029/2004GL021738.
Trenberth, K. E., and D. A. Paolino (1980), The Northern Hemisphere sea-level pressure data set: Trends, errors and discontinuities, *Mon. Weather Rev.*, *108*, 855–872.
Visbeck, M., E. P. Chassignet, R. G. Curry, T. L. Delworth, R. R. Dickson, and G. Krahmann (2003), The ocean's response to North Atlantic Oscillation variability, in *The North Atlantic Oscillation: Climatic Significance and Environmental Impact*, *Geophys. Monogr. Ser.*, vol. 134, edited by J. W. Hurrell et al., pp. 113–145, AGU, Washington, D. C.
von Storch, H., and F. W. Zwiers (1999), *Statistical Analysis in Climate Research*, Cambridge Univ. Press, New York.
Wallace, J. M., C. Smith, and Q. Jiang (1990), Spatial patterns of atmosphere-ocean interaction in the northern winter, *J. Clim.*, *3*, 990–998.
Walter, K., and H.-F. Graf (2002), On the changing nature of the regional connection between the North Atlantic Oscillation and sea surface temperature, *J. Geophys. Res.*, *107*(D17), 4338, doi:10.1029/2001JD000850.

T. Crueger and E. Zorita, GKSS Research Centre, Institute for Coastal Research, Geesthacht D-21494, Germany. (traute.crueger@zmaw.de)
H. Kuhnert and J. Pätzold, Department of Geosciences, University of Bremen, D-28334 Bremen, Germany.